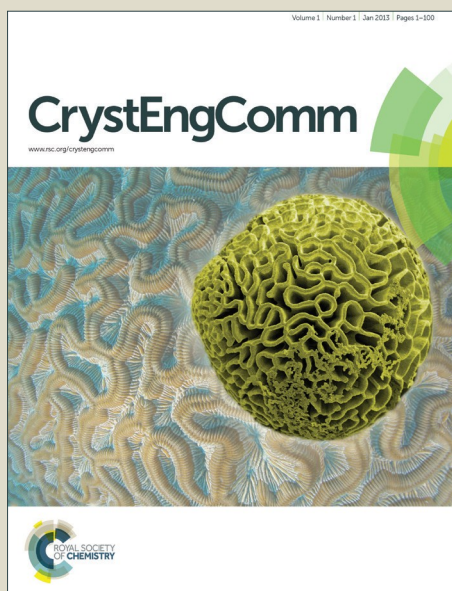


# CrystEngComm

Accepted Manuscript



This is an *Accepted Manuscript*, which has been through the Royal Society of Chemistry peer review process and has been accepted for publication.

*Accepted Manuscripts* are published online shortly after acceptance, before technical editing, formatting and proof reading. Using this free service, authors can make their results available to the community, in citable form, before we publish the edited article. We will replace this *Accepted Manuscript* with the edited and formatted *Advance Article* as soon as it is available.

You can find more information about *Accepted Manuscripts* in the [Information for Authors](#).

Please note that technical editing may introduce minor changes to the text and/or graphics, which may alter content. The journal's standard [Terms & Conditions](#) and the [Ethical guidelines](#) still apply. In no event shall the Royal Society of Chemistry be held responsible for any errors or omissions in this *Accepted Manuscript* or any consequences arising from the use of any information it contains.



## Hydrogen-bonding Networks of Purine Derivatives and Their Bilayers for Guest Intercalation

Yoona Jang,<sup>a</sup> Seo Yeon Yoo,<sup>b</sup> Hye Rin Gu,<sup>b</sup> Yu Jin Lee,<sup>b</sup> Young Shin Cha,<sup>b</sup> Laekyeong You,<sup>a</sup> Kyungkyou Noh<sup>a</sup> and Jaheon Kim<sup>\*a</sup>

Received 00th January 20xx,  
Accepted 00th January 20xx

DOI: 10.1039/x0xx00000x

www.rsc.org/

Two purin derivatives, 6-chloro-9-propyl-purin-2-amine (pr-GCl) and 6-chloro-9-pentyl-purin-2-amine (pt-GCl) have been synthesized and their crystal structures are determined by single crystal X-ray diffraction analyses. The purin rings in pr-GCl or pt-GCl form unique two-dimensional hydrogen-bonding networks which in turn stack with  $\pi$ - $\pi$  interactions to give bilayers covered with alkyl chains. In pt-GCl, the pentyl groups interact effectively among themselves so that void space for guest molecules is not available. In contrast, pr-GCl can form host-guest co-crystals. Nuclear magnetic resonance (NMR) analyses of the pr-GCl crystals immersed in various solvents up to 60 min indicate that aromatic molecules (benzene, xylene isomers) are better guests than aliphatic ones (*n*-hexane, cyclohexane, isooctane) in terms of their inclusion time and amounts. Powder X-ray diffraction (PXRD) patterns for the guest-included pr-GCl crystals produce quite different from a simulated one, supporting the guest diffusion into the pr-GCl crystals. The crystal structure of *p*-xylene@pr-GCl reveals that *p*-xylene molecules are intercalated between the characteristic pr-GCl bilayers that are shown in both pr-GCl and pt-GCl crystals.

### Introduction

Self-assembly of organic molecules via hydrogen-bonding is a reliable route to achieving well-defined structural architectures.<sup>1</sup> A prerequisite for this process is to devise appropriate building blocks which have complementary hydrogen-bonding donor and/or acceptor pairs. A molecule itself can act as both hydrogen-bonding donor and acceptor like trimesic acid.<sup>2</sup> In many situations, however, it is hard to predict what type of hydrogen-bonding networks will be given in crystalline lattice; for example, anhydrous guanine forms eight hydrogen bonds with three nearest neighbours to produce flat two-dimensional network.<sup>3</sup> In this regard, symmetrical and reliable donor/acceptor pairs are preferred as building blocks as demonstrated in cyanuric acid/melamine<sup>4</sup> or guanidinium/organic sulfonate (GS),<sup>5</sup> and so on.<sup>6</sup> It is notable that the GS pairs developed by Ward and co-workers give robust two-dimensional hydrogen-bonding networks with alternative arrays of positive hydrogen bond donors and negative acceptors, and can accommodate guest molecules between the hydrogen-bonding bilayers to form numerous host-guest complex crystals by introducing various pendant groups in organic sulfonates. Thus far, systems like the GS pairs are

rare which can retain their global architecture during guest-inclusion processes.<sup>5a</sup>

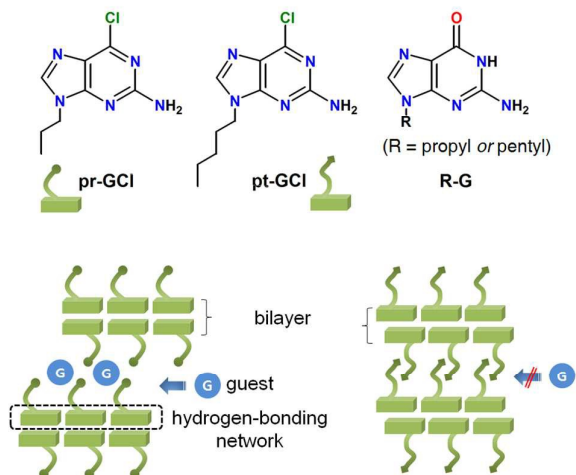
Recently, it has been shown that nucleobase such as uracil and thymine derivatives can form similar bilayers to the GS pairs.<sup>7</sup> For example, N<sup>1</sup>-hexyluracil or N<sup>1</sup>-hexylthymine molecules by themselves form flat two-dimensional hydrogen-bonding networks which in turn stack with other layers *via*  $\pi$ - $\pi$  interactions and their hexyl chains fill the space between the bilayers, which resembles a lipid bilayer.<sup>7a,b</sup> The overall feature could be retained when fluorouracil derivatives are crystallized<sup>7c</sup>; that is, the uracil ring is responsible for building hydrogen-bonding networks of which patterns are affected by the alkyl chains with or without terminal functional groups and concomitant various weak interactions. Interestingly, in the case of cytosine,<sup>7d</sup> its N<sup>1</sup>-hexyl derivative does not show the characteristic bilayer structure observed in both N<sup>1</sup>-hexylthymine and N<sup>1</sup>-hexyluracil, implying that the type of nucleobases may affect the formation of bilayer structures.

Here, we report our serendipitous finding that two alkylated purin derivatives, 6-chloro-9-propyl-purin-2-amine (termed pr-GCl) and 6-chloro-9-pentyl-purin-2-amine (termed pt-GCl) which are synthetic precursors of respective guanine derivatives (Scheme 1), can be also assembled into the bilayer structures by forming their unique hydrogen-bonding networks. Interestingly, pr-GCl can accommodate various guest molecules in crystals while pt-GCl does not. When pr-GCl is recrystallized in *p*-xylene, its crystal structure reveals that *p*-xylene molecules are intercalated in the bilayers of host pr-GCl molecules. This feature is similar to that observed in the host-guest co-crystals of a GS system.<sup>5</sup>

<sup>a</sup> Department of Chemistry, Soongsil University, Seoul 06978, Korea. Fax: +82 2 824 4383; Tel: +82 2 820 0459; E-mail: jaheon@ssu.ac.kr.

<sup>b</sup> Hankuk Academy of Foreign Studies, Yongin 17035, Korea.

† Electronic Supplementary Information (ESI) available: NMR and IR spectra, crystal pictures, crystal and refinement tables, ORTEP drawings, NMR spectra for guest@pr-GCl crystals, and PXRD patterns. CIF files: CCDC 1417638 (pr-GCl), 1417639 (pt-GCl), and 1417640 (*p*-xylene@pr-GCl). See DOI: 10.1039/x0xx00000x



Scheme 1. Purin derivatives and host bilayers in this work.

## Experimental section

### Synthetic procedures

The organic molecules in this work method were synthesized by a literature method with slight modifications.<sup>8</sup>

**6-Chloro-9-propyl-purin-2-amine (pr-GCl).** 6-Chloro-9H-purin-2-amine (1.00 g, 5.80 mmol) and  $K_2CO_3$  (1.20 g, 8.70 mmol) were dissolved in 20.0 mL of *N,N*-dimethylformamide. Into the homogeneous solution, 1-bromopropane (0.53 mL, 5.8 mmol) was added and the reaction mixture was stirred at room temperature for 10 hr. The reaction mixture was filtered to remove  $K_2CO_3$ , and solvent was evaporated by rotary evaporation to give a crude product. Finally, 6-chloro-9-propyl-purin-2-amine was isolated by column chromatography using EtOAc/n-hexane (10:1 v/v) as eluent (0.92 g, 4.36 mmol, 75% yield). For further analyses, pr-GCl was recrystallized in  $CH_2Cl_2$  by a simple evaporation method at room temperature. EA: Calcd. for  $C_8H_{10}ClN_5 \cdot (H_2O)_{0.25}(CH_2Cl_2)_{0.08}$ : C, 43.35; H, 4.84; N, 31.29%. Found: C, 43.45; H, 4.61; N, 31.32%.

**9-Propyl-Guanine (pr-G).** 6-Chloro-9-propyl-purin-2-amine (0.10 g, 0.47 mmol) was put in aqueous HCl solution (0.5 M, 90 mL). The reaction mixture was refluxed for 18 hr. The solution was cooled to room temperature, and 0.5 M aqueous NaOH solution was added dropwise to produce white precipitates. The white solid was filtered and washed thoroughly with deionized water, and dried in air. EA: Calcd. for  $C_8H_{11}N_5O$ : C, 49.73; H, 5.74; N, 36.25%. Found: C, 48.65; H, 5.66; N, 35.40%.

**6-Chloro-9-pentyl-purin-2-amine (pt-GCl).** 6-Chloro-9H-purin-2-amine (1.00 g, 5.80 mmol) and  $K_2CO_3$  (1.20 g, 8.70 mmol) were dissolved in 20.0 mL of DMF. Into the homogeneous solution, 1-bromopentane (0.88 mL, 5.8 mmol) was added and the reaction mixture was stirred at room temperature for 10 hr. The reaction mixture was filtered to remove  $K_2CO_3$ , and solvent was evaporated by rotary evaporation to give a crude product. Finally, 6-chloro-9-pentyl-purin-2-amine was isolated by column chromatography using EtOAc/n-hexane (10:1 v/v) as eluent (0.92 g, 4.36 mmol, 75% yield). For further analyses, pt-GCl was recrystallized in  $CH_2Cl_2$  by a

simple evaporation method at room temperature. EA: Calcd. for  $C_{10}H_{14}N_5Cl$ : C, 50.11; H, 5.89; N, 29.22%. Found: C, 49.95; H, 5.86; N, 28.78%.

**9-Pentyl-Guanine (pt-G).** 6-Chloro-9-pentyl-purin-2-amine (0.10 g, 0.43 mmol) was put in aqueous HCl solution (0.5 M, 90 mL). The reaction mixture was refluxed for 18 hr. The solution was cooled to room temperature, and 0.5 M aqueous NaOH solution was added dropwise to produce white precipitates. The white solid was filtered and washed thoroughly with deionized water, and dried in air. EA: Calcd. for  $C_{10}H_{14}ON_5 \cdot (H_2O)_{0.17}$ : C, 53.89; H, 6.90; N, 31.13%. Found: C, 53.14; H, 6.77; N, 30.61%.

### X-ray Crystallography

X-ray diffraction intensities were collected on a Bruker APEX CCD diffractometer using Mo  $K\alpha$  radiation ( $\lambda = 0.71075 \text{ \AA}$ ) at 173 K pr-GCl and 298 K for pt-GCl. Due to very thin crystal morphology, the x-ray data for *p*-xylene@pt-GCl was obtained at 173 K with a synchrotron light source ( $\lambda = 0.71000 \text{ \AA}$ ) on an ADSC Quantum-210 detector at 2D-SMC at the Pohang Accelerator Laboratory (PAL), Korea. Both pr-GCl and pt-GCl crystallize in a triclinic space group,  $P\bar{1}$  (No. 2) while *p*-xylene@pr-GCl belongs to an orthorhombic space group  $Ccca$  (No. 68, origin choice 2). Initial structures were solved by direct methods using SHELX-S and refined by full-matrix least-squares techniques against  $F^2$  with SHELXL-2013.<sup>9</sup> Four and eight independent molecules were respectively identified in pr-GCl and pt-GCl. In *p*-xylene@pr-GCl, two pr-GCl and two *p*-xylene molecules were defined as an asymmetric unit. One of two pr-GCl was disordered over two general sites with a same probability. The *p*-xylene molecules were also disordered over two sites at different inversion centres; that is, two independent molecules sit on different special positions (0.5, 0.5, 0.5) and (0.75, 0.75, 0.5), respectively. Disorder models for each *p*-xylene were built based on electron densities with avoiding possible guest-guest and guest-host bad contacts. Due to the very weak intensity data, the final R values for *p*-xylene@pr-GCl were quite high but the refined structure gave reasonable crystal packing and bond geometries. For pr-GCl, the occluded solvent molecules could not be identified due to diffuse electron densities. Therefore, the structural refinement was conducted by employing a SQUEEZE treatment within the PLATON software package.<sup>10</sup> All non-H atoms were refined anisotropically, and all H atoms were generated in ideal positions and included for the refinement processes. The space groups were checked by the ADDSYM routine of the PLATON.<sup>10</sup> Crystal and refinement data are listed in Tables S1 (pr-GCl), S3 (pt-GCl), and S5 (*p*-xylene@pr-GCl). The ORTEP drawings are displayed in Figures S12 (pr-GCl), S13 (pt-GCl), and S14 (*p*-xylene@pr-GCl).

## Results and discussion

### Crystal Structures of pr-GCl and pt-GCl

Alkylated purin derivatives in this work are prepared as precursors to their guanine forms as show in Scheme 1. Guanine (G), a base in DNA, can form stacked layers of two-dimensional hydrogen-bonding networks via  $\pi$ - $\pi$  interactions.<sup>3</sup> The layered structure is lost when G is functionalized with ethyl group and instead assembles into hydrogen-bonding tapes.<sup>11</sup>

Thus, our intention was to introduce longer alkyl chains, propyl or pentyl groups to G (abbreviated as pr-G or pt-G, respectively), and to investigate their crystal packing by single crystal X-ray diffraction (SCXRD) analyses. However, the obtained small microcrystals of R-Gs were not suitable for structure elucidation. Instead, we were interested in the crystal structures of pr-GCl and pt-GCl because they resemble their guanine forms in terms of shapes and potential hydrogen bonding ability.

While pt-GCl crystallizes without void space pr-GCl forms co-crystals with dichloromethane ( $\text{CH}_2\text{Cl}_2$ ) which was used as a solvent and detected in the  $^1\text{H-NMR}$  spectrum measured with dissolved crystals in  $\text{DMSO-}d_6$  (Fig. S1). It was not possible to identify the included dichloromethane based on the current X-ray data due to their severe disorder, requiring a SQUEEZE treatment.<sup>10</sup> In spite of this difference, the overall crystal packing is similar to each other. In both crystals, the purin rings form hydrogen-bonding with adjacent molecules to form almost flat layers which stack via  $\pi$ - $\pi$  interactions to give bilayers running parallel to the crystallographic *ac*-plane for pr-GCl and *bc*-plane for pt-GCl, respectively (Fig. 1a). In the pr-GCl crystal, a terminal ethyl moiety of the propyl group is positioned almost perpendicularly to the purine ring and the remaining ethylene ( $-\text{CH}_2-$ ) group attached to N is located nearly at the molecular plane (Fig. 1). The pentyl group in pt-GCl also behaves in a similar way. Thus, a bilayer is covered with alkyl chains on both sides, which is reminiscent of the bilayer of GS systems having pendant groups in organic sulfonates.<sup>5b</sup>

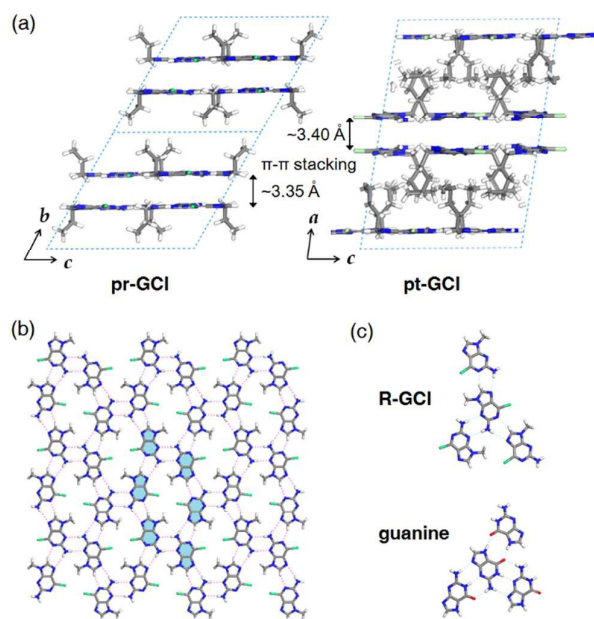


**Figure 1.** Crystal structures of (a) pr-GCl and pt-GCl are displayed with stick models. Colour codes: C, grey; H, white; N, blue; Cl, green. (b) Hydrogen-bonding network in a layer of pr-GCl or pt-GCl is shown with possible hydrogen bonds as dotted red lines. Only the  $-\text{CH}_2$  groups in propyl chains are drawn for simplicity. A hexamer unit is highlighted with coloured molecules. (c) The hydrogen bonds in pr-GCl (or pt-GCl) are compared with those in anhydrous guanine.

A hydrogen-bonding layer can be described as fused pseudo-hexagonal tiles, and a pr-GCl or pt-GCl molecule interacts with three neighbouring molecules via six possible hydrogen bonds (Fig. 1b). An amino group ( $-\text{NH}_2$ ) in the middle molecule is engaged in hydrogen bonds respectively with two  $\text{sp}^2$  N acceptors located in two different molecules; indeed, two N donor atoms in the middle pr-GCl molecule in turn interacts with two  $-\text{NH}_2$  groups in the neighbouring molecules. The H atom attached to the C atom in an imidazole ring interacts with a pyrimidine N atom via weak hydrogen-bonding. Interestingly, this hydrogen bonding pattern is similar to that observed in G; a central G interacts also with three nearest neighbours via hydrogen bonds in the crystal structure of anhydrous G (Fig. 1c).<sup>3</sup> However, G form a total of eight hydrogen bonds whereas pr-GCl or pt-GCl forms six because the Cl atom of R-GCl does not involve hydrogen bonding and the introduced alkyl groups prevent their bonded N atoms from participating in hydrogen bonds. It is notable that two Cl atoms are facing each other in the hexamer unit with an average Cl...Cl distance of 3.50 (pr-GCl) or 3.30 Å (pt-GCl) and an average bond angle of  $\sim 160^\circ$  around two Cl atoms ( $\angle \text{C-Cl}\dots\text{Cl}$ ). This arrangement is classified as the Type I halogen bonding.<sup>12</sup> However, at a Cl...Cl distance of 3.5 Å, the interaction energy is calculated to  $\sim 5$  kJ/mol,<sup>13</sup> which is small and thus not considered as a true halogen bonding.<sup>12</sup>

The local hydrogen-bonding fashion is almost same for pr-GCl and pt-GCl, the two layers in pr-GCl is less displaced from each other than those in pt-GCl: the distances between the centres of the hexamer units are 3.56 and 5.46 Å respectively in

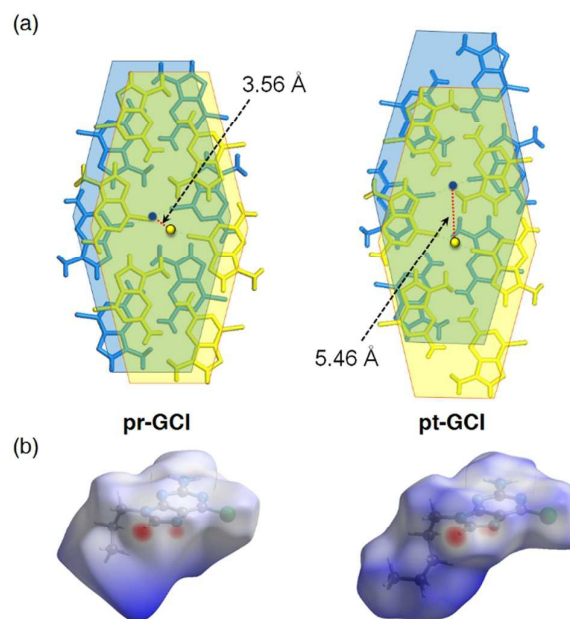


**Figure 2.** (a) The relative displacement of hexamer units in the  $\pi$ - $\pi$  stacked layers is compared: the upper and bottom layers are respectively coloured with yellow and blue, and the centres of each hexamers are marked as coloured dots. (b) Hirshfeld surfaces of pr-GCl and pt-GCl are shown. For simplicity, neighbouring molecules are not drawn.

pr-GCl and pt-GCl (Fig. 2a). This different displacement is mainly attributed to the guest included in pr-GCl. Calculations of Hirshfeld surfaces<sup>14</sup> indicate that only 73% of a molecular surface of pr-GCl contacts neighbouring pr-GCl whereas a pt-GCl molecule is completely enclosed (100%) by other pt-GCl molecules. That is, the remaining 27% of the pr-GCl surface is not touching its neighbours but the 'missing' dichloromethane in the crystal structure. In both structures, the H(a selected molecule)-H(other molecules) contacts are calculated as dominant contribution to crystal packing: 28/73 and 45/100% respectively for pr-GCl and pt-GCl (not shown). This indicates that the displacement of two  $\pi$ -stacked layers in a bilayer should be affected by the interactions among the alkyl chains or the interactions with included guest molecules if R-GCl forms host-guest co-crystals.

### Guest inclusion experiments in pr-GCl crystals

We conducted guest inclusion experiments with dried pr-GCl crystals. A typical procedure is as follows. Dried pr-GCl crystals (ca. 10 mg) were immersed in a 4 mL vial containing *n*-hexane (1.0 mL). A total of seven vials were prepared in this way. After 5, 10, 15, 20, 30, 45, and 60 min, the crystals in each batch were collected by filtration, washed quickly with *n*-hexane, and dried for 1 min in a gentle flow of N<sub>2</sub> stream. Each sample was dissolved in DMSO-*d*<sub>6</sub> (0.50 mL) to measure a <sup>1</sup>H-NMR spectrum, and the ratio of *n*-hexane/pr-GCl in moles was calculated based on the integration of identified signals (Figs. 3, S15). The potential guest molecules selected were aliphatic and aromatic solvent: *n*-hexane, cyclohexane, isooctane, benzene, *o*-xylene, *m*-xylene, and *p*-xylene. The host crystals in aromatic solvent were dissolved at ~25 °C. In the case of cyclohexane, the solvent became frozen due to its high melting point, 6.5 °C. Therefore, the experimental temperature was maintained at 20 °C employing a circulating chiller; at this temperature, crystals were stable.

The plot in Fig. 3 gives some information on the inclusion properties of the guests in a semi-quantitative manner. First, the aromatic solvents are better guests in pr-GCl crystals than the aliphatic ones in terms of inclusion time and amount. For instance, the amount of benzene included in 5 min was greater than that of cyclohexane by more than ten folds. Within each class of guests, small one such as benzene and cyclohexane are favoured than larger ones. It is also notable that *p*-xylene is included faster than other isomers, *o*- and *m*-xylenes, indicating that molecular shape can affect the inclusion process. However, it is not possible to explain at molecular level why certain guests are favoured over others. Thus, we measured the powder X-ray diffraction (PXRD) patterns of the sample crystals employed in the NMR measurements (60 min) in order to compare their patterns with that of pr-GCl host crystals (Fig. 4).

The PXRD pattern of pr-GCl host crystals grown in dichloromethane were measured as a reference and compared to the simulated one from the crystal structure (Fig. 4). Confusingly, pr-GCl crystals gave a different PXRD pattern from the simulated one from a crystal structure. In the simulated PXRD pattern, the peak at  $2\theta = 7.58^\circ$  corresponding to the crystallographic (010) plane is extremely dominant in

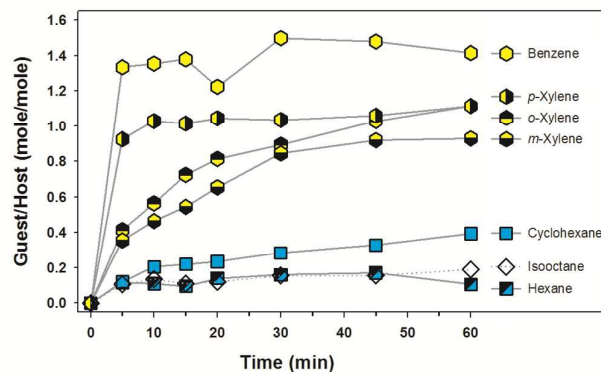


Fig. 3. Guest inclusion plot based on the <sup>1</sup>H-NMR analyses of the pr-GCl crystals immersed in solvent. Each point is the average value of two independent measurements.

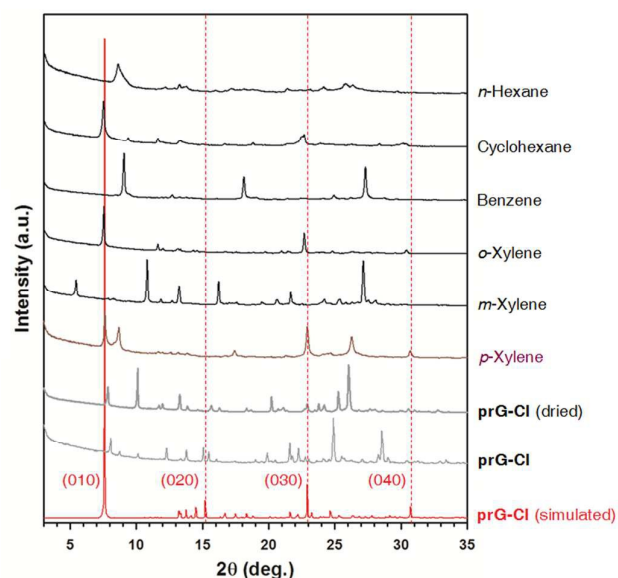
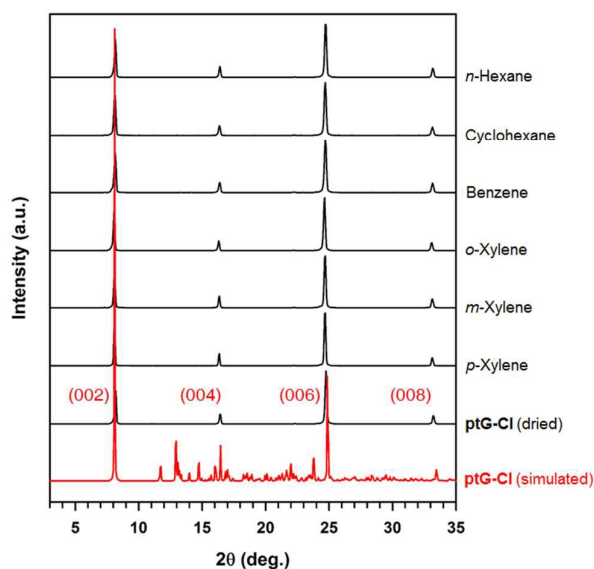


Fig. 4. PXRD patterns for pr-GCl and its guest-inclusion crystals are compared with the simulate one generated from the crystal structure of pr-GCl. The pr-GCl crystals were immersed for 1 h in each solvent listed on the plot before PXRD measurement.

intensities. However, in the PXRD pattern of pr-GCl crystals, the dominant peak was absent and instead other peaks appeared not found in the simulated pattern. Even, the fully 'dried pr-GCl' crystals gave a new pattern which is not matched to that of pr-GCl or the simulated pattern. The dominant peak in the simulated pattern is indicative of the well-ordered bilayers in crystals with a calculated d-spacing of (010) a 11.643 Å. Therefore, the disappearance of the peak in the measure patterns means that the bilayer stacking is not present any more in both dried and as-grown crystals, which is probably due to the fast escape of the dichloromethane guests when exposed to air.

Compared to host crystals, all solvent-included crystals showed simpler PXRD patterns (Fig. 4). In some crystals such as the pr-GCl crystals immersed in cyclohexane, *o*-xylene, or *p*-xylene exhibited relatively strong peaks whose diffraction angles are corresponding to (010) and (030) reflections observed in the simulated pattern. As these peaks are related to the regular separation of bilayers, it is suggested that the host-guest crystals would have similar packing modes as that observed in the pr-GCl crystal structure. In the benzene-included crystals, strong peaks shifted to higher diffraction angles. In contrast, the *m*-xylene-included crystals produced a peak at a lower angle,  $2\theta = 5^\circ$ . Unfortunately, when pr-GCl crystals are immersed in solvent, they cracked and became unsuitable for SCXRD studies (Fig. S11). Nevertheless, the changes in the PXRD patterns of the dried pr-GCl crystals upon guest inclusion strongly indicate that the pr-GCl host can have an ability of accommodating those guests by adjusting their relative locations in crystal lattice. However, without their crystal structures, it is hard to describe in detail the crystal packing of host and guest molecules in each case.

Indirect evidence for this suggestion is that the measured PXRD pattern for dried pt-GCl crystals was nicely matched to the simulated one from the crystal structure, indicating that pt-GCl layers are quite tightly packed and hardly disrupted: the strongest peak is attributed (002) at  $2\theta = 8.30^\circ$  and with a d-spacing value of 10.650 Å (Fig. 5). In order to further verify the dense packing nature of pt-GCl, guest-inclusion experiments were carried out using the same solvents used for pr-GCl: pt-GCl crystals (ca. 10 mg) were immersed at room temperature in each solvent (2.0 mL) for 1 day, and the collected samples were



**Fig. 5.** PXRD patterns for pt-GCl samples compared with the simulated one generated from the crystal structure of pt-GCl. The pr-GCl crystals were immersed for 1 day in each solvent listed on the plot before PXRD measurement. For clear comparison, the measured patterns were slightly shifted to the lower angle.

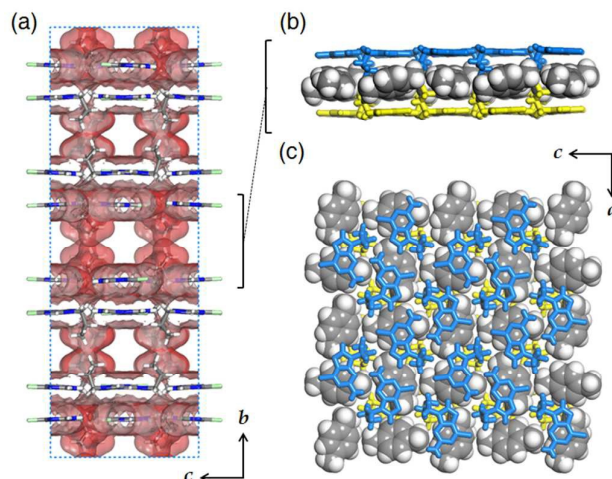


**Fig. 6** (a) Unit cell of recrystallized pr-GCl in *p*-xylene (*p*-xylene@pr-GCl) is shown with van der Waals surfaces of pr-GCl molecules. The empty space is occupied by disordered *p*-xylene molecules in crystals. (b) Selected pr-GCl layers are displayed with included *p*-xylene molecules. (c) A top view of (b) shows an array of the guest *p*-xylene molecules; *p*-xylene is disordered over two sites in the crystal structure, and one of the possible ordered arrays is presented.

analysed. As shown in the PXRD patterns in Fig. 5, all samples immersed in different solvents exhibited a same pattern, indicating that in pt-GCl crystal no available void space is present or the pentyl chains effectively packed among themselves do not allow any guest molecules to diffuse into the crystal lattice. This implies that the host property of the alkylated purin derivatives can be controlled by changing the length of the side chains with keeping the unique bilayer structures.

#### Structure of recrystallized pt-GCl in *p*-xylene

In order to obtain direct evidence on the above speculation, we tried to grow host-guest crystals directly in aromatic solvent. When aromatic solvent dissolving host crystals at about 25 °C was cooled to about 20 °C, guest-included pr-GCl crystals were obtained as very thin plates (Fig. S11). Except for the case of *p*-xylene, their measured PXRD patterns were well matched to those of the host-guest crystals prepared for the NMR experiments, that is, the pr-GCl crystals immersed in solvent (Fig. S16). As the crystals are so thin and aggregated, they became easily broken into parts when separated for crystal mounting for SCXRD experiments. After many trials, we managed to collect X-ray data for a single crystal obtained in *p*-xylene (*p*-xylene@pr-GCl) using synchrotron facility. Unfortunately, the data quality was not sufficient ( $R1 = 26\%$ ) but both pr-GCl and disordered *p*-xylene molecules could be identified successfully (Fig. S14). As seen in Fig. 6, pr-GCl molecules form bilayers between which *p*-xylene molecules are occluded. The bilayers are separated by 11.035 Å which is between 11.643 Å ( $\text{CH}_2\text{Cl}_2$ @pr-GCl) and 10.650 Å (pt-GCl). It is not understood why the simulated PXRD pattern was not matched to the measured one similarly to the case observed for pr-GCl (Fig. S16). Nevertheless, the crystal structure of *p*-xylene@pr-GCl structure shows that the hydrogen-bonding

networks by pr-GCl can be maintained and the characteristic bilayers can also work for intercalating guest molecules. This type of assembly may be regarded as an LSAM (long range synthon aufbau module) or a large synthon.<sup>12a</sup>

## Conclusions

In this work, 6-chloro-9-propyl-purin-2-amine (pr-GCl) molecules are assembled into two-dimensional hydrogen-bonding networks and in turn, form bilayers via  $\pi$ - $\pi$  stacking. The bilayers are coated with alkyl chains, and can intercalate various solvent molecules in crystalline states with keeping the unique hydrogen-bonding network. However, a similar molecule, 6-chloro-9-pentyl-purin-2-amine (pt-GCl) does not play a host role due to the dense packing of the pentyl chains between the bilayers. Thus, it is anticipated that R-GCl, which is functionalised with other alkyl or aryl groups, will show new guest-inclusion behaviours or recognise specific guest molecules not observed in pr-GCl.

## Acknowledgements

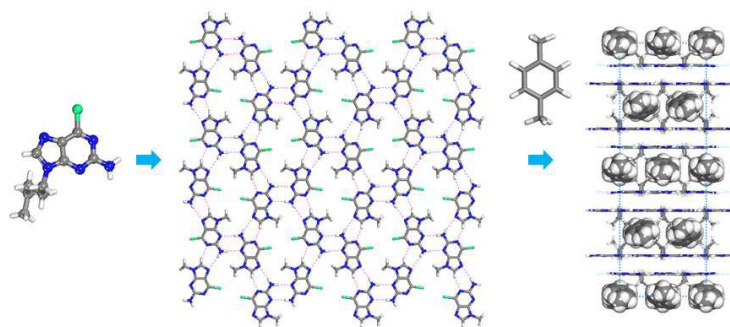
This research was supported by the Soongsil University Research Fund (No-201110000507). Single-crystal X-ray diffraction data for *p*-xylene@pr-GCl were collected using a synchrotron radiation facility at a beamline 2D-SMC of Pohang Accelerator Laboratory (PAL).

## Notes and references

- G. R. Desiraju, *Acc. Chem. Res.*, 2002, **35**, 565.
- S. V. Kolotuchin, E. E. Fenlon, S. R. Wilson, C. J. Loweth, S. C. Zimmerman, *Angew. Chem. Int. Ed. Engl.* 1995, **34**, 2654.
- K. Guille, W. Clegg, *Acta Cryst.* 2006, **C62**, o515.
- T. J. Prior, J. A. Armstrong, D. M. Benoit, K. L. Marshall, *CrystEngComm*, 2013, **15**, 5838.
- (a) A. C. Soegiarto, A. Comotti, M. D. Ward, *J. Am. Chem. Soc.*, 2010, **132**, 14603; (b) M. J. Horner, K. T. Holman, M. D. Ward, *J. Am. Chem. Soc.*, 2007, **129**, 14640; (c) K. T. Holman, A. M. Pivovar, M. D. Ward, *Science*, 2001, **294**, 1907.
- (a) T. C. W. Mak, C.-K. Lam, J. Han, Q. Li, F. Xue. In *Organic Crystal Engineering*; E. R. T. Tiekink, J. J. Vittal, M. J. Zaworotko, Eds.; Jhon Wiley & Sons, Ltd: Wiley, 2010; pp 239-312; (b) T. C. W. Mak, F. Xue, *J. Am. Chem. Soc.*, 2000, **122**, 9860; (c) S. Lie, T. Maris, J. D. Wuest, *Cryst. Growth Des.* 2014, **14**, 3658; (d) C. A. Zentner, H. W. H. Lai, J. T. Greenfield, R. A. Wiscons, M. Zeller, C. F. Campana, O. Talu, S. A. FitzGerald, J. L. C. Rowsell, *Chem. Commun.*, 2015, **51**, 11642; (e) M. E. Garah, R. C. Perone, A. S. Bonilla, S. Haar, M. Campitiello, R. Gutierrez, G. Cuniberti, S. Masiero, A. Ciesielski, P. Samori, *Chem. Commun.*, 2015, **51**, 11677
- (a) M. Barceló-Oliver, B. A. Baquero, A. Bauzá, A. García-Raso, A. Terrón, I. Mata, E. Molins, A. Frontera, *CrystEngComm*, 2012, **14**, 5777; (b) M. Barceló-Oliver, C. Estarellas, A. García-Raso, A. Terrón, A. Frontera, D. Quiñero, E. Molins, P. M. Deyà, *CrystEngComm*, 2010, **12**, 362; (c) M. Barceló-Oliver, C. Estarellas, A. García-Raso, A. Terrón, A. Frontera, D. Quiñero, I. Mata, E. Molins, P. M. Deyà, *CrystEngComm*, 2010, **12**, 3758; (d) M. Barceló-Oliver, A. Bauzá, B. A. Baquero, A. García-Raso, A. Terrón, E. Molins, A. Frontera, *Tetrahedron Lett.*, 2013, **54**, 5355.
- Y.-L. Wu, K. E. Brown, M. R. Wasielewski, *J. Am. Chem. Soc.* **2013**, **135**, 13322.
- (a) G. M. Sheldrick, SHELXS-97, Program for crystal structure analysis, University of Göttingen, Göttingen, Germany, 1997; (b) G. M. Sheldrick, SHELXL-2013 (version 2013/4), Programs for crystal

- structure analysis, University of Göttingen, Göttingen, Germany, 2013.
- A. L. Spek, PLATON, A Multipurpose Crystallographic Tool; Utrecht University: Utrecht, The Netherlands, 2011.
  - R. Destro, T. J. Kistenmacher, R. E. Marsh, *Acta Crystallogr., Sect. B* 1974, **30**, 79.
  - (a) A. Mukherjee, S. Tothadi, G. R. Desiraju, *Acc. Chem. Res.*, 2014, **47**, 2514; (b) G. R. Desiraju, P. S. Ho, L. Kloo, A. C. Legon, R. Marquardt, P. Metrangolo, P. Politzer, G. Resnati, K. Rissanen, *Pure Appl. Chem.*, 2013, **85**, 1711; (c) L. C. Gilday, S. W. Robinson, T. A. Barendt, M. J. Langton, B. R. Mullaney, P. D. Beer, *Chem. Rev.*, 2015, DOI: 10.1021/cr500674c.
  - M. V. Vener, A. V. Shishkina, A. A. Rykounov, V. G. Tsirelson, *J. Phys. Chem. A*, 2013, **117**, 8459.
  - (a) M. A. Spackman, J. J. McKinnon, *CrystEngComm*, 2002, **4**, 378; (b) M. A. Spackman, D. Jayatilaka, *CrystEngComm*, 2009, **11**, 19; (c) M. J. Bialek, J. K. Zaręba, J. Janczak, J. Zoń, *Cryst. Growth Des.*, 2013, **13**, 4039.

## Graphic Abstract



6-Chloro-9-propyl-purin-2-amine (pr-GCl) forms two-dimensional hydrogen-bonded networks which in turn stack via  $\pi$ - $\pi$  interactions, leading to bilayers that can accommodate organic guest molecules.